International Advance Journal of Engineering, Science and Management (IAJESM)
ISSN -2393-8048, January-June 2022, Submitted in February 2022, iajesm2014@gmail.com

Mathematical Modeling on Tumor Growth Research

John Abhishek Masih, Asstt. Professor, St. John's College Agra, Email: Jamsjc2703@Gmail.Com
Dr. Rajiv Philip, Associate Professor, Department of Mathematics, St. John's College, Agra
Manish Sharma, Department of Mathematics, L B S Degree College, Gonda

Abstract

There is a long history of simulating dynamic biological processes with mathematical models. Quantitative methods have also been used in cancer research within the last few decades. A growing array of mathematical, somatic, computational, and manufacturing methods have stood used to study different facets of tumour growth, by the eventual objective being to comprehend how the cancer inhabitants reacts to therapeutic involvement. The so-called "in silico trials," which forecast a patient's individual reply to different treatment combinations and sequencing or dose schedules, are quickly evolving into a vital tool for improving patient care. In this article, we outline the foundations of mathematical modelling of tumour growth and interactions with hosts, as well as a summary of some of the most important and groundbreaking methods.

Keywords: tumor modeling, angiogenesis

1. Introduction:

A potent tool for verifying experiments, testing theories, and simulating the dynamics of intricate systems is mathematical modelling. Mathematical models not only expedite the process of simulating complicated systems and aid in understanding its mechanistic foundations, but they also eliminate the need for costly laboratory tests and the associated biological variability. These models, specifically for oncology, can stand calibrated with untried or clinical statistics, and they can be used to assess competing theories of tumour evolution and comprehensively analyse treatment alternatives prior to clinical intervention. Quantitative modelling techniques are widely available, and a growing variety of theoretical attitudes are being functional to cancer biology with success. Near 20 years ago, distinct based cell models and ODE models unbolted the door to measureable cancer biology. An overview of the development of these models and their application in simulating tumour progression and treatment response is provided here. After that, we'll talk about a variety of models and their ability to predict and confirm aspects of cancer biology. Bodnar et al. (2016) proposed a personal of angiogenesis representations that is a simplification of the Hahnfel. Model, Measured personal of models contains of binary differential equations through distributed period delays. Xiao and Ruan (2007) analysis of the epidemic prototypical thru no monotone frequency rate. Yang and Xiao (2010) analysed the Influence of latent historical and nonlinear occurrence rate on the undercurrents of SIRS epidemiological representations. De Pillis et al. (2005) validated scientific model of cell-mediated immune reply to tumor development. Peirce (2008) studied on the Computational and Mathematical Modeling of Angiogenesis.

2. Ordinary differential equation (ODE) models of tumor growth

As of the continuous changes in period, it is challenging to determine the digit of cancer cells within a tumour. It is possible for tumour cells to divide, go dormant, or die. Therefore, characterising the quantity of tumour cells over time is extremely difficult. Formalising the projected changes in cell number with time, however, is not difficult. Living cell counts only vary in response to cell division or death.

Variance in *live* cell number terminated period intermission
= number of cells *formed* and *died* over stretch intermission

The calculated time variance, dt, determines how many and how frequently cells multiply as well as how many cells die (where d stands aimed at variance and t represents for time). Accept for the moment that a cancer cell has a 24-hour cell cycle. The likelihood of the cell dividing then approaches 100% finished the progression of a day. The likelihood that a cell will divide within an hour is 1/24, even in the absence of knowledge about the exact stage of the cell series at which cell is today. The aforementioned example can stand applied to the population level even in cases when the precise integer of cells in a tumour population is indefinite.

Aimed at a inhabitants of unsynchronized cells thru a cell cycle measurement of 24 hours we dismiss assume that entirely cells split once if dt=24 hrs. Correspondingly, if dt=1hr, individual a fraction of cells in the inhabitants is anticipated to division. One explanations similarly aimed at cell expiry. We consequently must announce the period difference as well as binary parameters keen on the upstairs equation: If dt=24 hours, then we can take on that completely cells in a inhabitants of unsynchronized cells by a 24-hour cell cycle divide once. In a similar vein, only a portion of the population—roughly 1/24—should split if dt=1 hour. One gives comparable explanations for cell death. As a result, we need to add two parameters and the time difference to the equation above:

$$\frac{difference\ in\ number\ of\ cells}{dt} = \alpha + \beta$$

where α and β represent the percentage of in-between and dying cells every day (dt), respectively, and hence represent the population-wide per capita growth and mortality rates. It goes without saying that after a proliferative event, the number of cells must increase, and following a cell death occurrence, it must decrease. Let's present the number of cells, or variable c. After that, the variance in cell number converts dc, and the equation upstairs can be expressed as follows:

$$\frac{dc}{dt} = \alpha c - \beta c \ (1)$$

Accept that there are one million cells, or c=106, at time t=0, or the beginning of the experiment. Dynamics of population expansion may take 1 of 3 paths: I When α = β, dc/dt equals 0. In this instance, the population shows signs of tumour dormancy and the digit of cells in the inhabitants remains constant. It is noteworthy that when α = β = 0, it indicates that every cell in the inhabitants is in a state of quiescence or dormancy. Conversely, when α = β > 0, cell death balances out cell multiplication. If (ii) α > β, dc/dt > 0 and the inhabitants of cells determination expand faster as a result of continuous growth at higher α-β rates. Conversely, if (iii) α < β and dc/dt < 0, the inhabitants resolve drop monotonically (fig. 1).

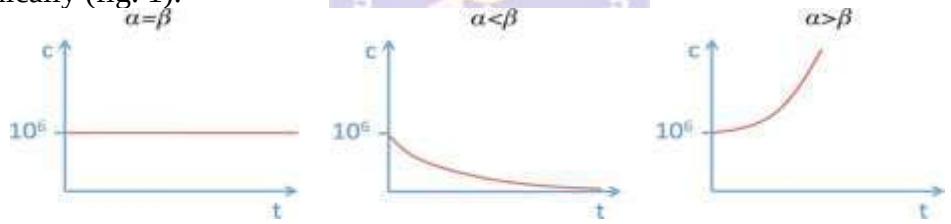

Fig. 1: Growing dynamics of the cell inhabitant's c over time t for various qualified rates

One can simplify Equation (1) to a one-parameter issue. We can merge the standings αc-βc into a sole term (α-β)c. Additionally, we announce a sole parameter, λ, where λ=α-β, denoted as the net inhabitants growth rate. Next, the ODE explaining the evolution of the cell inhabitants over period is:

$$\frac{dc}{dt} = \lambda c \ (2)$$

As previously, the population falls, stays the same, or rises, depending on whether λ<0; λ=0; λ>0. A model of this type can then be parameterized using experimental statistics since in vitro inhabitant's studies (fig. 2).

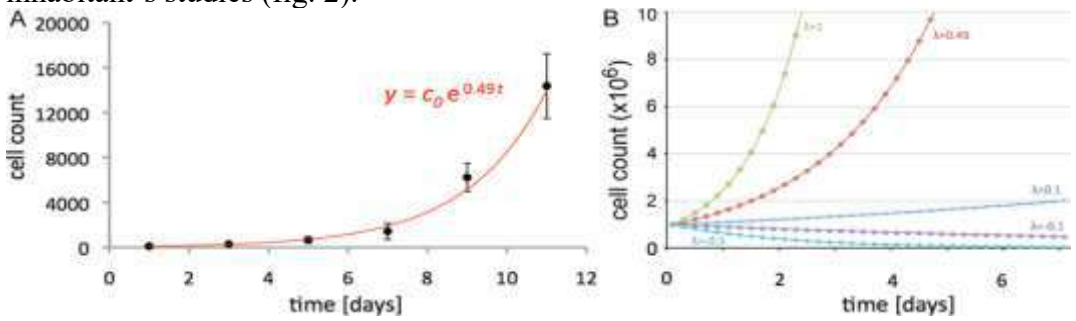

Fig. 2: Population growth results from a mathematical model

3. Dynamic tumor growth rates

When tumour growth is modelled using a relentless per capita evolution rate, carrying capacity restrictions are ignored and exponentially expanding cell populations result. Solid tumours develop quickly at first but slow down as they get bigger [11–14]. Consequently, rather than staying constant, the per capita frequency of tumour growth must to be based on the tumour extent c. The logistic model provides a well-known illustration of a per capita rate of tumour growth that depends on tumour size in relation to the host resonant size K. Fig. 3 expressions the development of inhabitants size as thriving as the growth rate in need of on inhabitants size relative to K aimed at changed parameters λ.

$$\frac{dc}{dt} = f(c)c$$

$$\frac{dc}{dt} = \lambda(c)\left\{1 - \frac{c}{k}\right\} \quad (3)$$

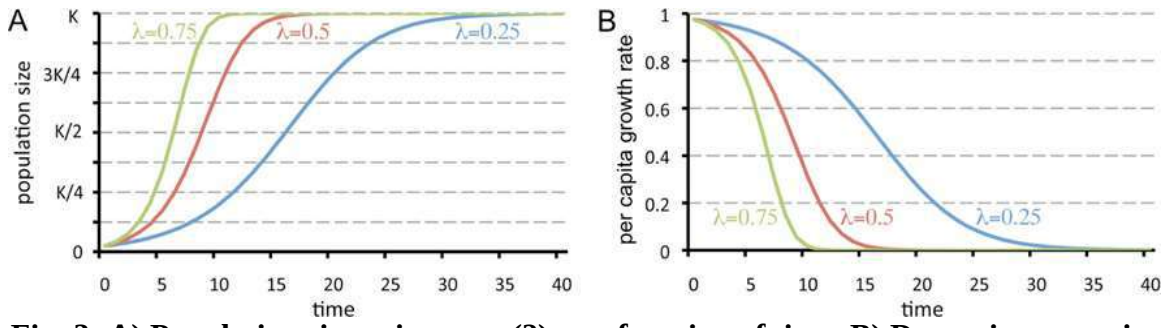

Fig. 3: A) Population size using eqn. (2) as a function of time. B) Dynamic per capita growth rates that correspond.

Many dynamic growth rate functions that are relevant to the growth of tumours have been discussed. It has been demonstrated that the so-called Gompertz curve can replicate biological growth, which slows down with population size. As a result, it can be used to explain the observed tumour development slowdown with tumour size. The growth rate can be calculated by dividing the carrying capacity by the negative logarithm of the current population size. Despite a extra rapid growth rate fall-off, inhabitants growth mimics that experimental by eqn. (3) and specified in fig. 3 (fig. 4).

$$\frac{dc}{dt} = -\lambda(c)log\left\{1 - \frac{c}{k}\right\} \quad (4)$$

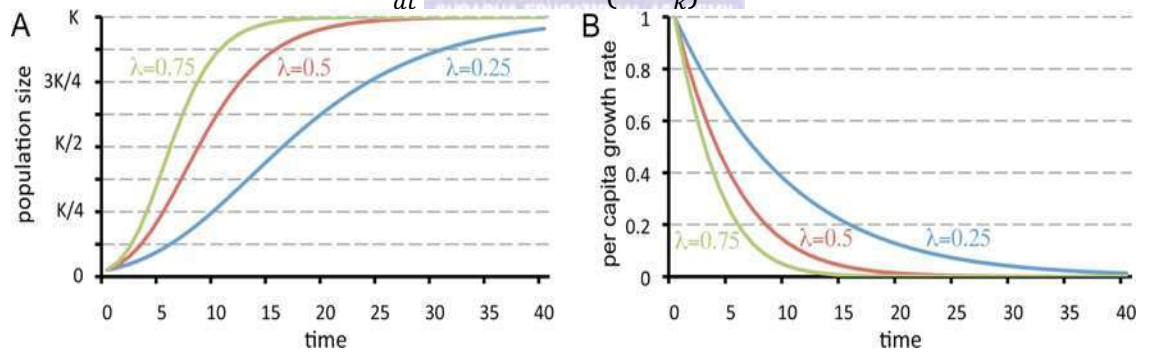

Fig. 4: A) Population size using eqn. (4) as a function of time. B) Dynamic per capita growth rates that correspond.

The carrying capacity itself may not be constant in a diseased environment. Depending on the size of the tumour, an increase in cell mass and physical pressure may cause the basement membranes to expand and distort, enhancing the tumor's spatial carrying capacity. On the other hand, tumour growth can also stop if the host vasculature fails to supply the growth hormones and nutrients that the tumour needs. Vascular dormancy limits the flow of nutrients and oxygen into the interior of the tumour, balancing both cell death and proliferation. The largest tumour size that can be sustained by circulatory supply is therefore determined by the carrying capacity. The tumour population interacts with the host vasculature through the release of pro- and anti-angiogenic agents, resulting in a carrying capacity K that varies over time. Hahnfeldt and associates deduced that vascular inhibition is related to the (tumour volume)2/3 using diffusion-consumption arguments.

$$\frac{dK}{dt} = \emptyset c - \emptyset K c^{2/3} \quad (5)$$

where ϕ and φ represent the constant, constructive rates of stimulation and inhibition, respectively, of angiogenesis. Tumour growth is initially encouraged by strong stimulation, but as the tumour enlarges, the inhibitory effects will become more pronounced than the stimulator, resulting in a plateau in the tumor's size and vascular supply (fig. 5).

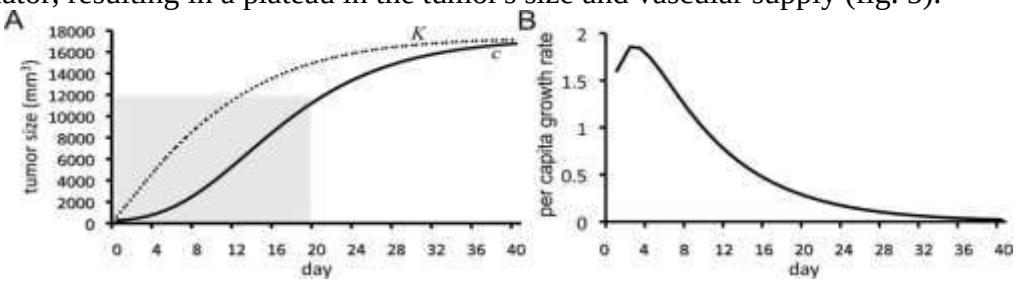

Fig. 5: tumor's dynamic carrying capacity during evolution

4. Modeling tumor treatment

There are two main approaches to treating tumours. One way to cause a significant decrease in tumour volume is to kill cancer cells that are still growing or to lower the tumor's support by lowering its carrying capacity. Differential equation models may easily encompass the impacts of both cancer therapy modalities. The updated Hahnfeldt model (eqns. (4) & (5)) will be examined now.

$$\frac{dK}{dt} = \emptyset c - \emptyset K c^{2/3} - \text{vKg(t)}$$

Chemotherapy or immunotherapy is examples of anti-tumor treatments that, in the most basic scenario, cause a continuous tumour cell kill with strength $0 \leq \xi \leq 1$. After the tumour has developed for 40 days, Figure 6 illustrates the tumor's response to various degrees of cell death (c.f. Figure 5). Hahnfeldt et al. modelled the drug's concentration (g(t), which includes partially cleared drug concentrations from prior administrations, as a function of the suppression of angiogenesis caused by administered anti-angiogenic drugs.

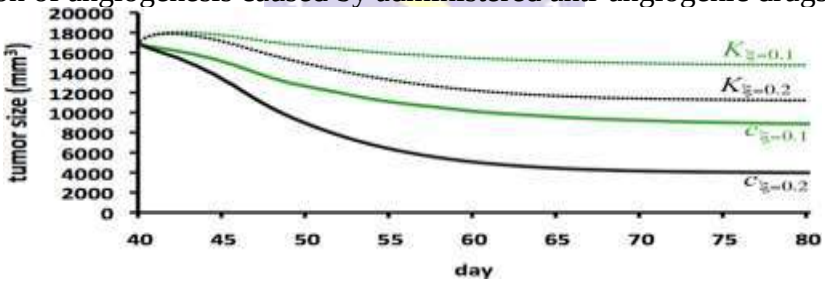

Fig. 6: Antitumor therapy for varying degrees of cell death ξ

5. Partial differential equation representations of tumor growth

While models based on ODE need shown to be a valuable tool for simulating the evolution of the total number of tumour cells over period, the maximum obvious drawback with this method is that it ignores spatial factors. Patients die not from the total amount of cancer cells in their figures, but rather from the local invasion of tissue by the primary tumours, which then spread (metastasize) to additional parts of the figure to form subordinate tumours. The primary cause of death for cancer patients is these metastatic tumours. Partial differential equation (PDE) models can be used to mimic two important phenomena that are intrinsically spatial: cancer invasion and metastatic dissemination. A population n in these models is often characterised as a density, or proportion of the maximum accessible volume at a given spatial point (x), (x,y), or (x,y,z) in one, dual, or three dimensions, individually. It is therefore scaled amid 0%-100%, or 0-1. The variable n now depends on disparities in the measured spatial dimensions in addition to changes in time t. The partial derivatives of its n involve the equation for n independent variables. Omitting the well-thought-out spatial domain, partial derivative of n $\frac{\partial n}{\partial t.}$

Tissue invasion is essential to the development and dissemination of cancer and is required for metastasis to be successful. Three main elements make up the invasion process: The cancer cells undergo three main processes: (i) they release different enzymes known as

matrix debasing enzymes (MDE); (ii) these MDEs break down the extracellular matrix (ECM); and (iii) the cancer cells aggressively migrate and proliferate into the immediate tissue. Inspired by former work by Gatenby, may have created the first geographic model of cancer assault. This model took into account how too many H+ ions could break down the surrounding tissue, creating a gap where cancer cells could spread and multiply. The spatiotemporal evolution of H+ ions, m, extracellular matrix (or standard host tissue), v, and cancer cells, c, is modelled by the following organization of PDE:

$$\frac{\partial c}{\partial t} = \nabla.(D_c(1-v)\nabla_c) + \rho c(1-c)$$

$$\frac{\partial m}{\partial t} = \nabla^2 m + \delta(c-m)$$

$$\frac{\partial v}{\partial t} = \mathrm{v}(1-\mathrm{v}) - \eta m v$$

where δ is the constant rate of creation of H+ ions, γ is the constant rate of extracellular matrix squalor, Dc is the continuous diffusion constant, and ひ is the endless rate of cancer cell explosion. As the aforementioned equations demonstrate, cancer cells multiply and undergo nonlinear diffusion, as well as secrete H+ ions that diffuse and cause the normal material to break down. In the nonattendance of cancer cells, the normal tissue is thought to grow logistically to return to its healthy state while the H+ ions also experience linear decline. We direct interested readers to partial differential equation textbooks for information on the population-level explanation of accidental cell migration, or diffusion, as it is mathematically expressed. Based on the previously indicated organization of PDE, Gatenby forecast the presence of a hypocellular opening at the boundary among normal and malignant tissue using a mix of mathematical analysis (travelling wave theory) and computational simulation. Hematoxylin-eosin stained micrographs of invasive tumours were later found to exhibit this (Fig. 7). H+ ions (blue circles) released by tumours (red triangles) disperse and break down healthy tissue (green squares) or the extracellular matrix. The growing tumour front and the receding tissue may be shown to be separated in the simulations (white arrows). B) As predicted by models, an H&E tarnished micrograph of tumor-host contact shows a hypocellular gap. This concept was expanded upon in later PDE models that used reaction-diffusion-taxis models to study the interactions, was found to be crucial to the migration of cancer cells. This was initially done by the Perumpanani model. The rate and depth of cancer cell penetration into the host tissue were predicted once more using a mix of travelling wave analysis and computer simulations. Cell proliferation was excluded from this continuum model in order to focus solely on the role that cancer cell migration plays in invasion. However, later in same work, cancer cell proliferation was included to the discrete version of the model (see the following section). Among the degrading enzymes that Chaplain, Lolas, and Andasari have studied in greater detail is the urokinase plasminogen system.

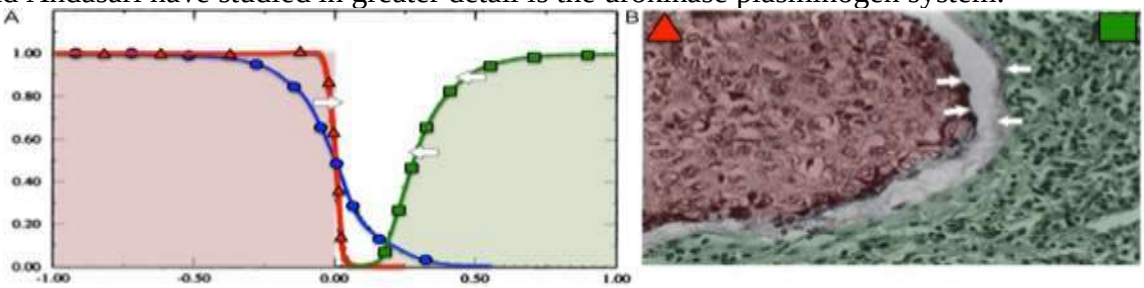

Fig. 7: Results from simulations and experimental evidence supporting cancer

While Gerisch and Chaplain and Chaplain employ a continuum model that includes cell-cell adhesion through a non-local integral term, Frieboes concentrate on cell-cell adhesion and employ a moving boundary approach. In Anderson's research, which was the first to employ a two-dimensional context to examine the role of haptotaxis specifically, the extracellular matrix (ECM) of the tissue was explored:

$$\frac{\partial c}{\partial t} = \nabla.(D_c(1-v)\nabla_c) + \rho c(1-c)$$

$$\frac{\partial m}{\partial t} = \nabla^2 m + \delta(c - m)$$

$$\frac{\partial v}{\partial t} = \mathrm{v}(1 - \mathrm{v}) - \eta m v$$

The findings of this model's computational simulation investigated the finding that discrete cancer cells can spread past a malignant tissue's "visible margin," which is "detectable" to surgeons. This work may have been the first to investigate the relationship between probability and stochastic events in invasion models. A sample outcome of the discrete model computation simulation in a two-dimensional environment is displayed in Figure 8. The specific cancer cells are multiplying and relocating within the newly formed area (via diffusion and haptotaxis), secreting degrading enzymes. The image illustrates how the discrete model's stochastic nature results in a deterministic PDE model would not anticipate that distinct cancer cells could mathematically enter the standard tissue to a further degree. The ability to take into account events at the level of different cells is one benefit detached models have over continuum models. Various phenotypic characteristics and significant events like mutations can be considered with discrete models. The advent of discrete models has also prompted the creation of "multiscale models," in which parameters at the cellular level can be connected to intracellular occurrences through the use of systems of ordinary differential equations.

6. Conclusion:

Over the past few decades, a growing number of scientific models have been included into cancer study. Here, we've demonstrated how basic quantitative models can stand secondhand to simulate intricate biological progressions and communications by demonstrating how they're produced and contrasted with experimental data. We have selected foundational works. As examples, and have been forced to omit a substantial amount of outstanding mathematical modelling material in the interest of simplicity.

7. References:

1. Yang, Y, Xiao, D (2010). Influence of latent period and nonlinear incidence rate on the dynamics of SIRS epidemiological models. *Discrete Contin. Dyn. Syst., Ser. B* 13, 195-211.
2. De Pillis, LG, Radunskaya AE and Wiseman CL, (2005). A validated mathematical model of cell-mediated immune response to tumor growth. *Cancer research*, 65(17), 7950-7958.
3. Bodnar M and Piotrowska M J. (2016). Stability analysis of the family of tumour angiogenesis models with distributed time delays. *Commun Nonlinear Sci Numer Simulat*., 124–142.
4. Xiao, D, Ruan, S (2007). Global analysis of an epidemic model with nonmonotone incidence rate. *Math. Biosci.* 208, 419-429.
5. Peirce S M. (2008). Computational and Mathematical Modeling of Angiogenesis. *Microcirculation*, 15(8), 739–751.
6. Al-Maweri, Sadeq & Addas, Abdallah & Tarakji, Bassel & Abbas, Alkasem & Al-Shamiri, Hashem & Alaizari, Nader & Shugaa-Addin, Bassam. (2014). Public Awareness and Knowledge of Oral Cancer in Yemen. Asian Pacific journal of cancer prevention : APJCP. 15. 10861-5. 10.7314/APJCP.2014.15.24.10861.
7. Bhoopathi, Praveen & Reddy, Peddi & Kotha, Arpitha & Mancherla, Monica & Boinapalli, Prathibha & Samba, Amit. (2014). Oral health related knowledge, attitude and practices among the primary health care workers of a district in India. Journal of International Society of Preventive & Community Dentistry. 4. S11-S17. 10.4103/2231-0762.144563.
8. Sawlani K, Kumari N, Mishra AK, Agrawal U (2014) Oral Cancer Prevalence in a Tertiary Care Hospital in India. J Family Med Community Health 1(4): 1022.